

Received Date : 16-Jun-2016

Revised Date : 16-Aug-2016

Accepted Date : 29-Aug-2016

Article type : Original Papers

Tau imaging with [¹⁸F]THK-5351 in progressive supranuclear palsy

Aiko Ishiki, MD, PhD¹, Ryuichi Harada, PhD², Nobuyuki Okamura, MD, PhD^{3,4}, Naoki Tomita, MD, PhD, MPH¹, Christopher C. Rowe, MD, PhD⁵, Victor L. Villemagne, MD, PhD^{5,6}, Kazuhiko Yanai, MD, PhD³, Yukitsuka Kudo, MD, PhD², Hiroyuki Arai, MD, PhD¹, Katsutoshi Furukawa, MD, PhD^{1,7}

1. Department of Geriatrics and Gerontology, Institute of Development, Aging and Cancer, Tohoku University, 4-1 Seiryomachi, Aobaku, Sendai, Japan

2. Division of Neuro-imaging, Institute of Development, Aging and Cancer, Tohoku University, 4-1 Seiryomachi, Aobaku, Sendai, Japan

3. Department of Pharmacology, Tohoku University School of Medicine, 2-1 Seiryomachi, Aobaku, Sendai, Japan

4. Division of Pharmacology, Faculty of Medicine, Tohoku Medical and Pharmaceutical University 4-4-1 Komatsushima, Aobaku, Sendai, Japan.

5. Centre for PET, Austin Health, 145 Studley Road, PO Box 5555

This is the author manuscript accepted for publication and has undergone full peer review but has not been through the copyediting, typesetting, pagination and proofreading process, which may lead to differences between this version and the [Version of Record](#). Please cite this article as [doi: 10.1111/ene.13164](https://doi.org/10.1111/ene.13164)

This article is protected by copyright. All rights reserved

Heidelberg Victoria, Australia 3084

6. *The Florey Institute of Neuroscience and Mental Health, The University of Melbourne, 30 Royal Parade, Parkville, VIC 3052 Australia*

7. *Division of Community of Medicine, Faculty of Medicine, Tohoku Medical and Pharmaceutical University. 1-12-1 Fukumuro, Miyaginoku, Sendai, Japan*

Corresponding author:

Katsutoshi Furukawa, M.D., Ph.D.

Division of Community of Medicine, Faculty of Medicine,
Tohoku Medical and Pharmaceutical University.

1-12-1 Fukumuro, Miyaginoku, Sendai, Miyagi 983-8512, Japan.

Phone: 81-22-259-1221 FAX: 81-22-259-0507

E-mail: kfurukawa-ns@umin.ac.jp

Running title: Tau-PET imaging in PSP

Disclosure: No potential conflict of interest relevant to this article was reported.

Keywords: progressive supranuclear palsy, tau, PET

Abstract

Background: Visualization of pathogenic protein aggregates is crucial to elucidate pathomechanisms and to make accurate diagnosis in many neurodegenerative conditions. Aggregates of the microtubule-binding protein, tau, are one of the most important pathogenic molecules in neurodegenerative disorders. Progressive supranuclear palsy (PSP) is characterized by the deposition of tau proteins in some specific area such as the basal ganglia and the brainstem. We tried to detect tau lesions in the brains of the living patients with PSP with a novel PET tracer, [¹⁸F]THK-5351, which we recently developed.

Methods: Paraffin-embedded brain sections of the PSP patient were used for autoradiography with [^3H]THK-5351 and immunohistochemistry. Nine healthy controls (HCs), thirteen patients with AD, and three patients with PSP participated in this PET study with [^{18}F]THK-5351. To detect amyloid β deposition, PET imaging with Pittsburgh compound B (PIB) was also performed.

Results Autoradiography in the brain sections of patients with PSP demonstrated [^3H]THK-5351 binding to tau deposits with a high selectivity. Although PSP patients exhibited no remarkable [^{18}F]THK-5351 retention in the temporal cortex, significantly higher tracer retention was observed in the globus pallidus and midbrain. In contrast, amyloid imaging with PIB, showed no remarkable accumulation in the cerebral cortex of PSP.

Conclusions: We conclude that [^{18}F]THK-5351 PET can potentially be used to detect the regional brain distribution of tau lesions in PSP, therefore facilitating the differential diagnosis of neurodegenerative disorders associated with tau protein.

Introduction

Tau is a microtubule-binding protein that has been reported to be a key molecule in the pathogenesis of several neurodegenerative disorders causing dementia¹⁻³.

Neurodegenerative disorders in which tau is deposited in the brain are called “tauopathies”⁴.

Different morphologies of tau aggregates are observed, including neurofibrillary tangles (NFTs), tufted astrocytes (TAs), coiled bodies (CBs), and threads (Th) pathology^{4,5}.

Alzheimer’s disease (AD) is the most prevalent tauopathy, while all the other ones are grouped as “non-AD tauopathies.” Senile plaques and neurofibrillary tangles formed from amyloid β peptide ($\text{A}\beta$) and tau, respectively, are the major neuropathological hallmarks of

AD⁶. To elucidate the neurodegenerative mechanisms, imaging technology has been

developed to identify these misfolded and aggregated proteins in living patients. For over a

decade now, PET imaging has allowed visualization of amyloid plaques with $\text{A}\beta$ -PET tracers

This article is protected by copyright. All rights reserved

such as Pittsburgh Compound B (PIB) among others^{7,8}. Recently, several tau imaging radiotracers have been developed and used in clinical studies⁹⁻¹³. Moreover, we have recently developed a novel PET tracer, [¹⁸F]THK-5351, which can detect tau pathology in living patients with AD with a high degree of sensitivity and specificity¹⁴.

Progressive supranuclear palsy (PSP), characterized by deposition of 4-repeat (4R) tau isoforms in neuronal and glial inclusions in PSP¹⁵, is one of the most common non-AD tauopathies, manifesting as cognitive impairment, parkinsonism, gait instability, and disturbance of vertical eye movement^{4,5}. Postmortem studies in PSP revealed that the subthalamic nucleus, midbrain, and globus pallidus are the regions where tau deposits are most frequently observed^{4,5}. Clinically, PSP is divided into three categories (i.e., classic Richardson's syndrome [RS], PSP-parkinsonism [PSP-P], and pure akinesia with gait freezing [PAGF])^{4,5}. Molecular imaging studies to detect tau pathology, however, have rarely been performed in PSP so far. The visualization of tau deposits in living patients with PSP is crucial for the understanding and elucidation of the pathophysiological mechanisms of this disorder. Furthermore, because therapeutic drugs targeting tau for tauopathies such as AD and PSP are now under development¹⁶, the non-invasive detection and quantification of tau deposits in the brain is indispensable. In the present study, we studied if/how PET imaging with the tau-tracer, [¹⁸F]THK-5351, could detect tau deposits in patients with PSP.

Methods

Autoradiography, fluorescence staining, and immunohistochemistry in postmortem brain tissues

All experiments were performed under the regulations of the Ethics Committee of Tohoku University School of Medicine and the Austin Health. Brain samples from a patient with PSP (67-year-old male) were obtained from the Tohoku University Brain Bank. Paraffin-embedded brain sections were used for autoradiography and immunohistochemistry

This article is protected by copyright. All rights reserved

(IHC). For autoradiography, the brain sections were incubated with 3 nM [³H]THK-5351, and then briefly washed with PBS containing 10% ethanol. The autoradiographic images were obtained using an FLA-7000 phosphorimaging instrument (GE Healthcare). For the fluorescence staining, tissue sections were immersed in 100 μM THK-5351 solution containing 50% ethanol.

Adjacent sections were immunostained with an AT8 anti-tau monoclonal antibody (Innogenetics, Ghent, Belgium) or stained using a modified Gallyas-Braak method [17].

Radiosynthesis of the PET tracers for clinical PET study

Injectable solutions of [¹⁸F]THK-5351 were prepared with a radiochemical purity of >95% and a specific activity of 357 ± 270 GBq/μmol. [¹¹C]PIB was synthesized via a loop method using ¹¹C-methyl triflate. Injectable solutions of [¹¹C]PIB were obtained with a radiochemical purity of >95 % and a specific activity of 240 ± 48 GBq/μmol.

Clinical PET and MRI studies

Nine healthy controls (HCs), thirteen patients with AD, and three patients with PSP participated in this study. The demographic information of the study subjects were summarized in Table 1.. Written, informed consent was obtained from the patients or their guardians under standard ethical guidelines. The clinical diagnosis of probable PSP was based on the criteria of the National Institute on Aging-Alzheimer's Association¹⁸ and the National Institute of Neurological Disorders and Stroke and the Society for PSP¹⁹. A mini-mental state examination (MMSE)²⁰ and PSP rating scales²¹ were used to assess global cognitive and physical performance.

Magnetic resonance scans were performed using a SIGNA 1.5T machine (General Electric, Milwaukee, WI)¹². [¹⁸F]THK-5351 and [¹¹C]PIB PET scans were performed using an Eminence STARGATE scanner (Shimadzu, Kyoto, Japan). After delivering an intravenous

injection of 185 MBq of [¹⁸F]THK-5351 or 296 MBq of [¹¹C]PIB, dynamic PET images were obtained for 60 min ([¹⁸F]THK-5351) or 70 min ([¹¹C]PIB).

Image analysis

Standardized uptake value (SUV) images of [¹⁸F]THK-5351 and [¹¹C]PIB were obtained by normalizing the tissue radioactivity concentration to the injected dose and body weight. The analysis of the automated volumes of interest (VOI) was performed using the PNEURO module in the PMOD software (version 3.6; PMOD Technologies, Zurich, Switzerland)²². VOIs were defined in the following regions: parahippocampus, fusiform gyrus, middle and inferior temporal, orbitofrontal, posterior cingulate, lateral occipital, superior parietal, inferior and superior frontal, putamen, globus pallidus, midbrain, and the cerebellar cortex. The cerebellar cortex was used as a reference region. The ratio of the regional SUV to the cerebellar cortex SUV (SUVR) from 50 to 60 min post-injection was used as an index of [¹⁸F]THK-5351 retention. The neocortical A β burden was expressed as the average PIB SUVR for the following cortical VOIs: the ventrolateral prefrontal; parietal; superior and inferior temporal; and posterior cingulate cortices. Furthermore, the Z-scores were computed as follows: $z = [(individual\ value) - (HC\ mean)] / (HC\ SD)$.

Results

Biochemical characteristics and autoradiographic studies of THK-5351

In vitro autoradiograms of the brain sections were initially performed to examine the ability of THK-5351 to bind tau lesions in PSP (Fig. 1). In the PSP midbrain sections, a strong [³H]THK-5351 signal was observed that highly corresponded to the tau lesions identified by IHC (Fig. 1A and B). Furthermore, a microautoradiography of these sections indicated that there was a selective binding of [¹⁸F]THK-5351 to TAs (Fig.1 C and C inset).

Tau deposits stained with AT8 IHC matched the [³H]THK-5351 microautoradiography signal (Fig. 1C and D). Furthermore, the strong binding of THK-5351 to tau deposits in the striatum of the PSP case was additionally demonstrated by fluorescence microscopy (Fig. 1E).

Moreover, the fluorescent staining images with THK-5351 completely corresponded to the tau lesions detected with Gallyas–Braak staining (Fig. 1F).

[¹⁸F]THK-5351 PET studies in patients with PSP

PET scans with [¹⁸F]THK-5351 and [¹¹C]PIB, and MRI scans were performed in the patients with PSP as follows:

Patient 1: An 83-year-old right-handed male. He started to manifest cognitive impairment, including memory disturbance and disorientation three years before the PET scans. His standing and gait became unstable one year after the cognitive disturbance was observed. The appearance of extrapyramidal signs, such as muscle rigidity and akinesia, also coincided with the observation of the gait instability and disturbance. When the PET scans were obtained, he was bed-ridden and unable to stand or walk. Up and down gazes were restricted in his eye movement. His MMSE scores were 24 and 1 at the first visit (three years before the PET scans) and at the time of the PET scans, respectively. His PSP rating scale was 82 when the PET scans were performed. This patient exhibited the typical “hummingbird sign” on the MRI sagittal section, indicating significant atrophy of the midbrain.

[¹⁸F]THK-5351 PET scan showed high tracer retention in the globus pallidus ($z = 2.99$) and the midbrain ($z = 4.76$) (Fig. 2). High [¹⁸F]THK-5351 retention was additionally observed in the precentral ($z = 3.40$), superior parietal ($z = 4.65$), posterior cingulate ($z = 2.88$), and lateral occipital ($z = 3.23$) cortices in this patient. No remarkable retention of [¹⁸F]THK-5351 was observed in the parahippocampal gyrus ($z = 1.64$) or the inferior temporal cortex ($z = 1.42$). Furthermore, no remarkable retention of [¹¹C]PIB was observed in the neocortex of this patient.

Patient 2: A 78-year-old right-handed male. He presented with unstable gait two years before the PET scans. Early symptoms included memory impairment, disorientation, bradykinesia, dysphagia, and falls. When the [¹⁸F]THK-5351 and [¹¹C]PIB PET scans were obtained, patient presented with dyskinesia, vertical gaze palsy, muscle rigidity, akinesia, and retropulsion. His MMSE scores were 24 and 21 at the first visit (two years before the PET scans) and at the time of the PET scans, respectively. His PSP rating scale was 43 when the PET scans were obtained. A sagittal MRI showed the typical “hummingbird sign.”

[¹⁸F]THK-5351 PET images showed significantly higher tracer retention than controls in the globus pallidus ($z = 3.73$) and the midbrain ($z = 4.83$) (Fig. 2). High [¹⁸F]THK-5351 retention was additionally observed in the precentral ($z = 2.28$), superior parietal ($z = 3.00$), posterior cingulate ($z = 2.77$), and lateral occipital ($z = 2.43$) cortices. However, no remarkable retention of [¹⁸F]THK-5351 was observed in the parahippocampal gyrus ($z = 0.21$) and inferior temporal cortex ($z = 0.42$). Mild [¹¹C]PIB retention was observed in the neocortex (neocortical SUVR 1.54).

Patient 3: A 74-year-old right handed male. He developed some stiffness in his lower back three–four years before the PET scans. The patient also developed a posture of looking upwards, typical of PSP. After these initial symptoms, patient started developing some degree of unsteadiness in his gait. During this period, some difficulty in reading with diplopia and restricted eye movement appeared. Over the subsequent three years, he experienced a gradual worsening in balance, and wide based gait as he started to fall. He presented a quite marked restricted up and down gaze and saccadic interruption to smooth pursuit on the lateral gaze at the time of the PET scans. His recent scores of the MMSE and PSP rating scales were 28 and 78, respectively. An MRI scan indicated that his midbrain was atrophic, in addition to age-related volume loss throughout the entire brain. [¹⁸F]THK-5351 PET imaging resulted in a significantly high retention in the midbrain ($z = 3.98$) and globus pallidus ($z = 1.81$) in this subject. However, no remarkable retention of [¹⁸F]THK-5351 was observed in the neocortex.

The three patients that participated in the present study were diagnosed as probable PSP due to their gradually progressive symptoms, age of onset (>40 years), vertical supranuclear gaze palsy, and prominent postural instability with falls appearing on the first year of onset. In contrast with the HC and AD groups, a significantly higher [^{18}F]THK-5351 retention was observed in the globus pallidus and midbrain of patients with PSP (Table 2). The brain regional distribution of [^{18}F]THK-5351 retention in these PSP patients was completely different from the [^{18}F]THK-5351 retention pattern in AD patients. Specifically, the middle and inferior temporal cortex, fusiform gyrus, and parahippocampal gyrus, where high [^{18}F]THK-5351 retention was observed in AD, did not exhibit significant [^{18}F]THK-5351 retention in the PSP patients.

Discussion

To elucidate the pathogenesis of neurodegenerative disorders, non-invasive molecular imaging of aggregated proteins has been available for several years. Imaging of tau aggregates was not possible until recently. Therefore, neurodegenerative disorders except for AD, such as non-AD tauopathies could not be assessed by non-invasive approaches such as molecular imaging. Here, we describe a novel tau-PET tracer, [^{18}F]THK-5351, and examined the most representative non-AD tauopathy, PSP. As mentioned before, tau deposits in PSP are classified into NFTs, TAs, CBs, and Th, and they are predominantly prominent in subthalamic nuclei, substantia nigra, and globus pallidus^{4,5}. The present autoradiographical study indicated that THK-5351 can detect TAs very clearly.

All the PSP patients in the present study were deemed to be classic RS, because all of them exhibited supranuclear vertical gaze palsy and gait instability more prominently than parkinsonism or akinesia with gait freezing. The significant detection of tau lesions in the globus pallidus and the midbrain with [^{18}F]THK-5351 is in agreement with the neuropathological findings of classic RS^{4,5}. To confirm these finding, precise comparative

analyses between ante-mortem PET images and post-mortem neuropathological examination will be required. Moreover, investigations towards characterizing the ability of [¹⁸F]THK-5351 to further distinguish between PSP clinical presentations (RS, PSP-P, and PAGF) are warranted.

Non-invasive molecular imaging for the detection of proteinopathies is crucial for the investigation of the pathomechanisms and accurate diagnosis in neurodegenerative disorders. Beyond AD and PSP, it is extremely important to explore the utility of [¹⁸F]THK-5351 in the assessment of other non-AD tauopathies such as frontotemporal lobar degeneration, corticobasal degeneration, chronic traumatic encephalopathy or argyrophilic grain disease. Imaging-to-autopsy correlational studies will be necessary to validate the results presented here. In conclusion, [¹⁸F]THK-5351 is showing promise as a tau imaging tracer that will help elucidate the pathophysiological mechanisms underlying AD and non-AD tauopathies, allowing earlier and more accurate differential diagnosis, as well as assisting in subject recruitment, target engagement and efficacy monitoring in disease-specific anti-tau therapeutic trials.

Disclosure of the source of funding

The costs of publication of this article were defrayed in part by the payment of page charges. Therefore, and solely to indicate this fact, this article is hereby marked “advertisement” in accordance with 18 USC section 1734. This study was supported by research funds from GE Healthcare; the SEI (Sumitomo Electric Industries, Ltd.) Group CSR Foundation; the Industrial Technology Research grant program of the NEDO in Japan (09E51025a); Health and Labor Sciences Research grants from the Ministry of Health, Labor, and Welfare of Japan; grant-in-aid for Scientific Research (B) (15H04900); grant-in-aid for Scientific Research on Innovative Areas (Brain Protein Aging and Dementia Control) (26117003); grant-in-aid for Young Scientists (B) (15K19767); and grant-in-aid for JSPS

This article is protected by copyright. All rights reserved

Fellows and “Japan Advanced Molecular Imaging Program (J-AMP)” of the Ministry of Education, Culture, Sports, Science and Technology (MEXT), Japan.

References

- (1) Villemagne VL, Fodero-Tavoletti MT, Masters CL, Rowe CC. Tau imaging: early progress and future directions. *Lancet Neurol.* 2015; 14: 114-124.
- (2) Villemagne VL, Okamura N. In vivo tau imaging: obstacles and progress. *Alzheimers Dement.* 2014 10 (3 Suppl):S254-264.
- (3) James OG, Doraiswamy PM, Borges-Neto S. PET Imaging of Tau Pathology in Alzheimer's Disease and Tauopathies. *Front Neurol.* 2015; 6: 38. doi: 10.3389/fneur.2015.00038. eCollection
- (4) Williams DR. Tauopathies: classification and clinical update on neurodegenerative diseases associated with microtubule-associated protein tau. *Intern Med J.* 2006; 36: 652-660.
- (5) Williams DR, Holton JL, Strand C, et al. Pathological tau burden and distribution distinguishes progressive supranuclear palsy-parkinsonism from Richardson's syndrome. *Brain* 2007; 130: 1566-1576.
- (6) Villemagne VL, Chételat G, Neuroimaging biomarkers in Alzheimer's disease and other dementias. *Ageing Res Rev.* 2016; S1568-1637.
- (7) Klunk WE, et al. Imaging brain amyloid in Alzheimer's disease with Pittsburgh Compound-B. *Ann Neurol.* 2004; 55: 306-319.
- (8) George N, Gean EG, Nandi A, Frolov B, Zaidi E Advances in CNS Imaging Agents: Focus on PET and SPECT Tracers in Experimental and Clinical Use. *CNS Drugs.*

2015; 29: 313-330.

- (9) Maruyama M, et al. Shimada H, Suhara T, et al. Imaging of tau pathology in a tauopathy mouse model and in Alzheimer patients compared to normal controls. *Neuron*. 2013; 79: 1094-1108.
- (10) Chien DT, Bahri S, Szardenings AK et al. Early clinical PET imaging results with the novel PHF-tau radioligand [F-18]-T807. *J Alzheimers Dis*. 2013; 34: 457-468.
- (11) Okamura N, Furumoto S, Fodero-Tavoletti MT, et al. Non-invasive assessment of Alzheimer's disease neurofibrillary pathology using ¹⁸F-THK5105 PET. *Brain*. 2014; 137: 1762-1771.
- (12) Harada R, Okamura N, Furumoto S, et al. [¹⁸F]THK-5117 PET for assessing neurofibrillary pathology in Alzheimer's disease. *Eur J Nucl Med Mol Imaging*. 2015; 42: 1052-1061.
- (13) Johnson KA, Schultz A, Betensky RA et al. Tau PET imaging in aging and early Alzheimer's disease. *Ann Neurol*. 2016; 79:110-119.
- (14) Harada R, Okamura N, Furumoto S, et al. ¹⁸F-THK5351: A Novel PET Radiotracer for Imaging Neurofibrillary Pathology in Alzheimer's Disease. *J Nucl Med*. 2016; 57: 208-214.
- (15) de Silva R, Lashley T, Gibb G, Hanger D. Pathological inclusion bodies in tauopathies contain distinct complements of tau with three or four microtubule-binding repeat domains as demonstrated by new specific monoclonal antibodies. *Neuropathol Appl Neurobiol*. 2003; 29: 288-302.
- (16) Kumar A, Nisha CM, Silakari C, et al. Current and novel therapeutic molecules and targets in Alzheimer's disease. *J Formos Med Assoc*. 2015; 25. pii: S0929-6646(15)

00149-00147.

- (17) Ikeda K, Akiyama H, Kondo H, Haga C. A study of dementia with argyrophilic grains. Possible cytoskeletal abnormality in dendrospinal portion of neurons and oligodendroglia. *Acta Neuropathol (Berlin)*. 1995; 89: 409-414.
- (18) McKhann GM, Knopman DS, Chertkow H, et al. The diagnosis of dementia due to Alzheimer's disease: recommendations from the National Institute on Aging-Alzheimer's Association workgroups on diagnostic guidelines for Alzheimer's disease. *Alzheimers Dement*. 2011; 7: 263-269.
- (19) Litvan I, Agid Y, Calne D, et al. Clinical research criteria for the diagnosis of progressive supranuclear palsy (Steele-Richardson-Olszewski syndrome): report of the NINDS-SPSP international workshop. *Neurology*. 1996 47:1-9.
- (20) Folstein MF, Folstein SE, McHugh PR. "Mini-mental state". A practical method for grading the cognitive state of patients for the clinician. *J Psychiatr Res*. 1975; 12:189-198.
- (21) Golbe LI, Ohman-Strickland PA. A clinical rating scale for progressive supranuclear palsy. *Brain*. 2007; 130(Pt 6):1552-1565.
- (22) Ishiki A, Okamura N, Furukawa K, et al. Longitudinal Assessment of Tau Pathology in Patients with Alzheimer's Disease Using [¹⁸F]THK-5117 Positron Emission Tomography. *PLoS One*. 2015; 10: e0140311.

Table 1: Demographic information of the subjects

N	M/F	Age (mean +/- SD)	MMSE (mean +/- SD)
---	-----	-------------------	--------------------

HC	9	5/4	71.6 +/- 6.6	28.6 +/- 1.5
AD	13	9/4	76.6 +/- 9.1	19.2 +/- 4.2
PSP	3	3/0	78.3 +/- 3.7	16.7 +/- 11.4

HC: healthy control, AD: Alzheimer's disease, PSP: Progressive supranuclear palsy

MMSE: Mini-mental state examination

Table 2: Regional [¹⁸F]THK-5351 SUVRs, Z-scores and effect size

	SUVR						Z-score				Cohen's d	
	HC		PSP		AD		PSP		AD		PS	A
											P	D
Parahippocampal	2.03	± 0.12	1.94	± 0.14	2.61	± 0.24	0.93	± 0.72	4.89	± 2.04	1.13	2.87
Fusiform	1.83	± 0.18	1.85	± 0.10	2.36	± 0.27	0.36	± 0.28	3.00	± 1.54	0.05	2.22
Inferior temporal	1.52	± 0.13	1.56	± 0.17	2.10	± 0.27	0.88	± 0.50	4.37	± 2.05	0.22	2.56
Orbitofrontal	1.71	± 0.16	1.65	± 0.23	1.96	± 0.21	1.04	± 0.67	1.69	± 1.17	0.46	3.30
Posterior cingulate	1.48	± 0.12	1.72	± 0.41	1.83	± 0.12	1.99	± 0.45	2.90	± 0.97	0.50	2.95
Lateral	1.0	± 0.1	1.0	± 0.1	1.0	± 0.1	1.0	± 1.3	3.0	± 2.0	1.1	1.1

occipital	21	10	40	20	56	22	91	64	49	14	32	97
Superior	1.	0.	1.	0.	1.	0.	2.	1.	3.	1.	1.	2.
parietal	25	09	51	28	56	12	86	87	34	26	33	88
Inferior	1.	0.	1.	0.	1.	0.	1.	0.	1.	0.	0.	1.
frontal	25	10	41	14	40	13	48	22	66	95	79	26
Superior	1.	0.	1.	0.	1.	0.	1.	0.	1.	0.	0.	1.
frontal	23	13	42	23	42	12	46	47	43	88	55	52
Putamen	2.	0.	3.	0.	2.	0.	1.	0.	0.	0.	0.	0.
Globus	62	36	06	48	79	41	24	92	96	73	89	43
pallidum	3.	0.	4.	0.	3.	0.	2.	0.	0.	0.	2.	0.
Midbrain	24	42	42	57	38	41	84	97	86	54	40	35
	2.	0.	3.	0.	2.	0.	4.	0.	1.	0.	5.	0.
	56	18	38	20	49	32	53	47	52	83	33	24

Figure legends

Fig. 1. In vitro analyses of THK-5351 in autopsied samples

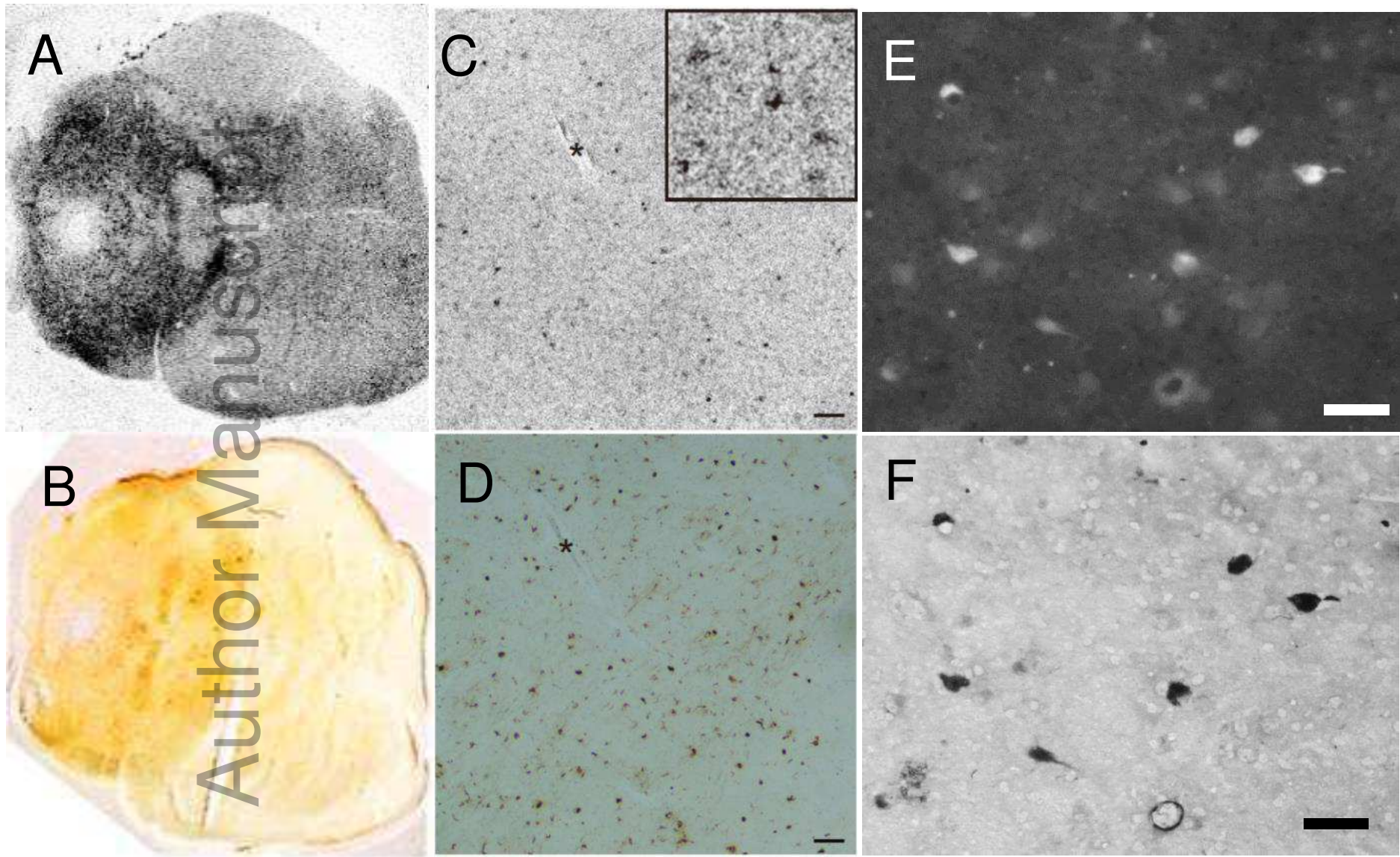
(A-F) In vitro autoradiography of [³H]THK-5351 and immunohistochemistry of the midbrain sections of progressive supranuclear palsy (PSP). Autoradiography images obtained using [³H]THK-5351, for the midbrain section of PSP (A), and the microautoradiography image of the midbrain of PSP (C) are presented in the upper panels. Immunohistochemical images with an anti-tau antibody, AT8, in the adjacent sections to (A) and (C) are presented in the lower panels (B) and (D), respectively. (E, F) Microscopic images of THK-5351 binding to tau lesions in PSP. (E) THK-5351 staining of the striatum from a patient with PSP. (F) Gallyas-Braak staining in the adjacent section.

Fig. 2. PET imaging with [^{18}F]THK-5351 in the subjects with healthy control, PSP and Alzheimer's disease

Representative axial, sagittal, and coronal [^{18}F]THK-5351 PET images from a healthy control subject (81-year-old female), three patients with progressive supranuclear palsy (PSP) and a patient with Alzheimer's disease (78-year-old male, MMSE score 13), showing significant higher retention [^{18}F]THK-5351 in the pallidum and midbrain of patients with PSP.

Fig. 3. PET imaging with [^{11}C]Pittsburgh compound B (PIB) in the subjects with healthy control and progressive supranuclear palsy (PSP)

[^{11}C]PIB images from a healthy control subject (81-year-old female) and two patients with PSP (patient 1 and 2).



This article is protected by copyright. All rights reserved.

Figure 1

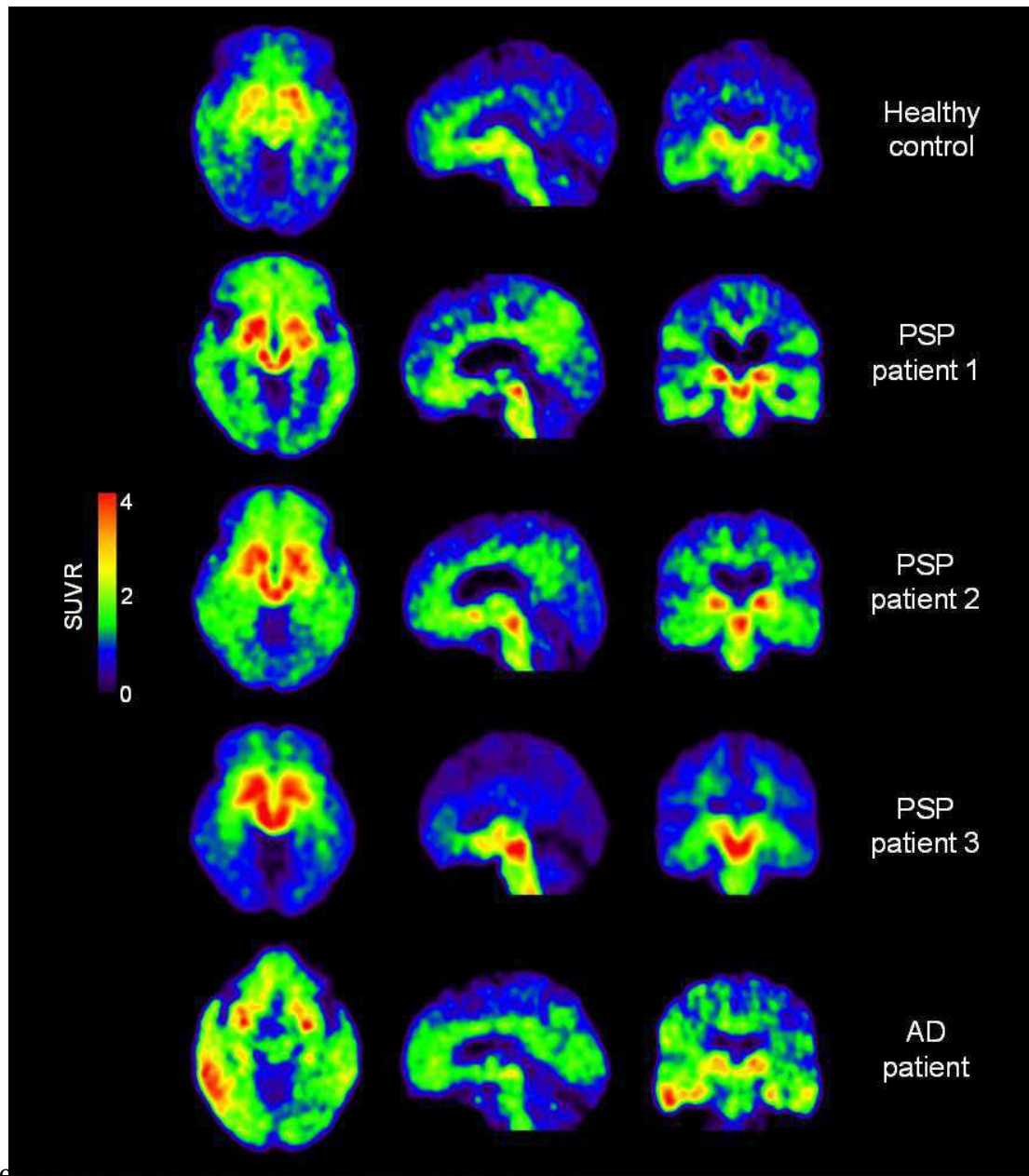


Figure 2

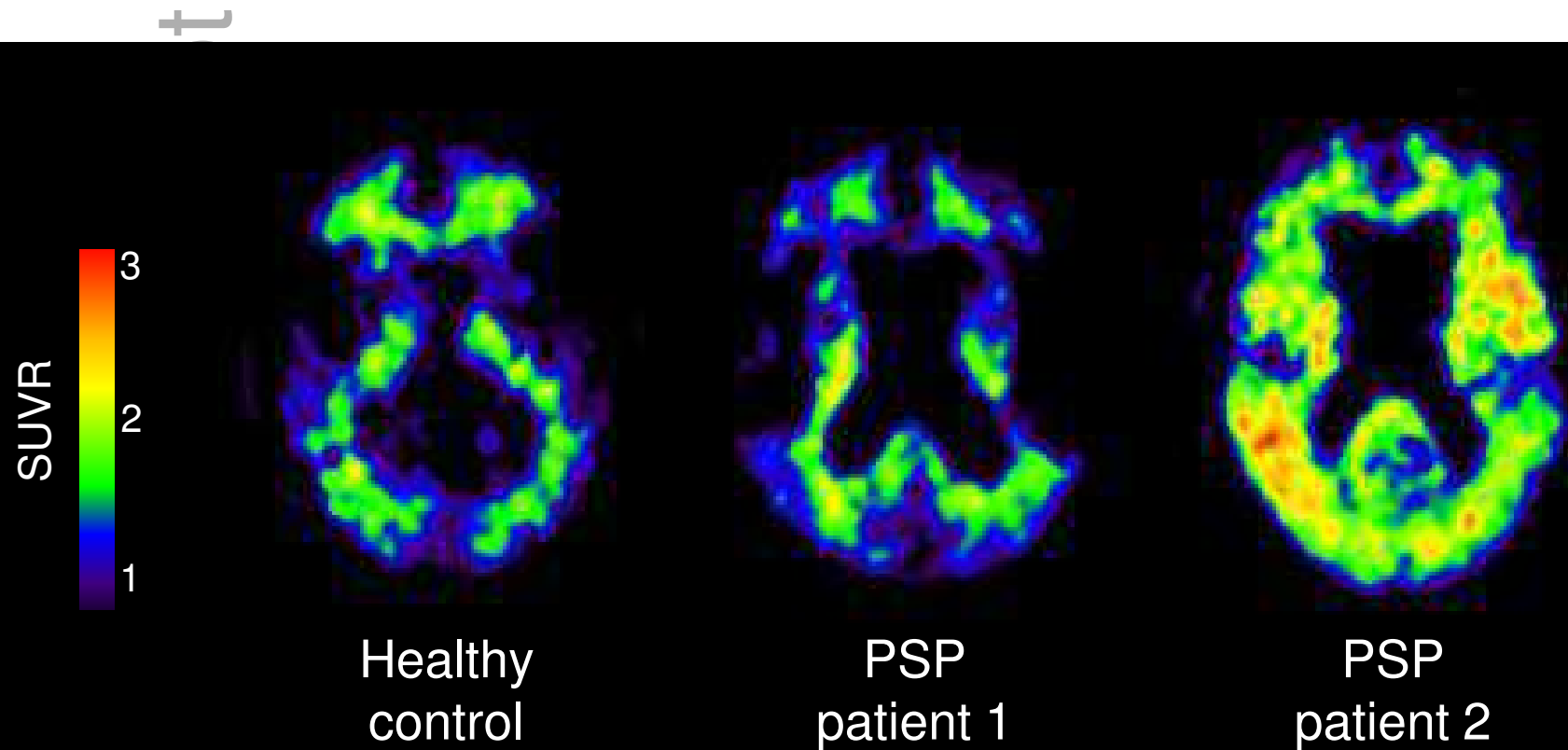


Figure 3